Chapter 1
Rotorcraft Aerodynamics

George Barakos

Abstract This chapter introduces the reader to the aerodynamic aspects of rotary wings. It is written as an introduction for aspiring students, not as a replacement of well-known texts used for rotorcraft classes at University level. It should be used as a first read what is a very complex but fascinating topic in rotorcraft. This chapter illustrates the aerodynamic environment of the rotor, the rotorcraft blade sections and their features, modern aerofoil developments, advanced blade tip designs and advanced rotor design methods. While studying this chapter, one should keep in mind that aerodynamics means different things to different people. When looking at pilot training, the lines between aerodynamics, performance, and aircraft handling are blurred. The technical literature on rotorcraft aerodynamics is dominated by the rotor, but there is a volume of work on fuselage drag as well.

Nomenclature

a_1, b_1	Amplitudes in flap angle equation, Eq. 1.11
A_1, B_1	Amplitudes in blade pitch equation, Eq. 1.5
A	Area
c	Blade chord
C_L	Lift coefficient
C_{Lmax}	Maximum lift coefficient
C_M	Pitching moment
C_T	Thrust coefficient
D	Aerodynamic drag
M	Mach number
M_{tip}	Tip Mach number
r_x	Fraction of the rotor radius

Supplementary Information The online version contains supplementary material available at https://doi.org/10.1007/978-3-031-12437-2_1.

G. Barakos (✉)
School of Engineering, University of Glasgow, Glasgow, Scotland
e-mail: george.barakos@glasgow.ac.uk

A. Filippone and G. Barakos (eds.), *Lecture Notes in Rotorcraft Engineering*,
Springer Aerospace Technology, https://doi.org/10.1007/978-3-031-12437-2_1

R	Rotor radius
R	Gas constant in Eq. 1.14
t	Time
T	Air temperature in Eq. 1.14
U	Air speed
U_p	Out-of-plane (perpendicular) velocity component
U_t	In-plane (parallel) velocity component

Greek Symbols

α	Angle of attack
β	Flap angle
γ	Forward tilt angle of the rotor; ratio between specific heats
λ_i	Inflow ratio
μ	Advance ratio
θ	Pitch angle
θ_o	Collective pitch
ϕ	Inflow angle
ρ	Air density
σ	Rotor solidity
ψ	Azimuth angle
ω	Angular frequency
Ω	Rotor angular speed

1.1 Introduction

This chapter will describe the rotor aerodynamic environment, its physics and flow conditions. It will then move to a historic approach where milestones in our understanding of how rotor aerodynamics work will be briefly presented. Key phenomena dominating rotor flows like dynamic pitch of the blades, variation of Mach number and operation within stall are then to be detailed. Each aspect of the rotor aerodynamics will be addressed using modern results and a combination of evidence from experimentation and simulation. Leaving the sectional aerodynamics, the chapter will progress in the effect of blade planform and how sectional and planform effects are combined to improve rotor performance. There are small practical MATLAB scripts that are used throughout the chapter to allow students to explore the covered effects and develop a better feel of the order of magnitude of the various effects. The chapter closes with a review of modern approached to automate the blade design or employ active structures and element like flaps, tabs, morphing etc.

Rotary wings are used everywhere in aerospace engineering and are nowadays very sophisticated devices designed and optimised with state of the art computer-based methods. At the same time rotary wings are the subject of wind-tunnel inves-

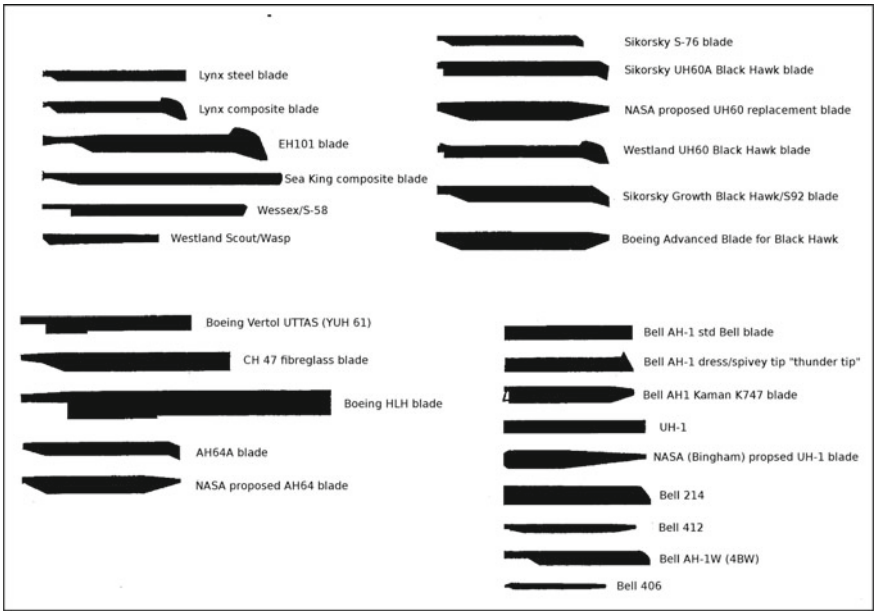

Fig. 1.1 Selection of rotorcraft blade planforms

tigations where very sophisticated flow measurement devices are used to help engineers identify key fluid mechanics phenomena (stall, vortex shedding etc.) that dictate the performance we can obtain when deploying these wings in applications. More interestingly, in recent years, a shift is observed in the research where acoustics is now taking centre stage next to efficiency trying to support the overall objectives of low environmental impact from aircraft.

Typical examples of rotary wing planforms used for helicopters are shown in Fig. 1.1 below where one may observe the lack of a universal trend in design. The main reason for this is the complex aerodynamic environment where rotary wings have to operate within and this will be discussed in the next section.

1.2 The Rotor Aerodynamic Environment

The aerodynamics of a rotor in hover or forward flight is complicated. A useful dimensionless speed which can be used to describe the occurring phenomena is the advance ratio μ defined as:

$$\mu = \frac{U}{\Omega R} = \frac{U}{U_{tip}} \tag{1.1}$$

which is the ratio of flight speed U to tip speed ΩR of a rotary wing of radius R, rotating about a centre of rotation at an angular speed Ω. For most helicopters the

advance ratio can reach values up to $\mu = 0.4$. As a typical example, most helicopters operate with tip speeds approximately in the range of 190–220 m/s; $\mu = 0.4$ indicates that the helicopter forward speed of ~80 m/s or 290 km/h for a tip speed of nearly 210 m/s. Most times we are interested in the velocities contributing to the advance ratio in a direction tangential to the rotor disk and perpendicular to it. This projection makes theoretical analyses easier and is used in several textbooks. Most of the times an $x - z$ system of reference is employed with x tangential to the rotor and z pointing through the disk.

$$\mu_x = \mu \cos\gamma, \qquad \mu_z = \mu \sin\gamma \tag{1.2}$$

where γ is the forward tilt angle of the rotor in radians. Another convention is that the rotor turns anti-clockwise as viewed from above, and the zero of the blade azimuth angle ψ is assumed to be at the back of the disk (6 O'clock). The rotor blade tangential velocity changes from root to tip and around the azimuth during a blade rotation.

$$U_t = U_{tip}\,[r_x + \mu \sin(\omega t)] \tag{1.3}$$

$$\psi = \omega t \tag{1.4}$$

and r_x is the fraction of the rotor radius, varying between 0 (at the centre) to 1 (at the blade tip). Also, t is time and ω is the rate of rotation. The normal velocity U_p of the air through the rotor disk depends on the disk tilt/orientation, the flapping speed of the blades, and the inflow to the rotor. A simple MATLAB script can be used to plot the tangential velocities over the rotor disk (see Fig. 1.2) for a given advance ratio. It is evident that there are different velocities on the advancing (higher velocity) and retreading (lower velocity) sides and as the blade rotates around the azimuth different amounts of lift will be generated on the two sides of the rotor. Consequently, unless the blades pitch and flap as they rotate the rotor alone will not be balanced, trimmed, and will give an unstable and uncontrollable aircraft. Based on the plots shown here, the aircraft will roll to the left.

The most common method to resolve this problem is by trimming the rotor the blades by varying their pitch angle, via what is called the swashplate mechanism, with its associated rotor head assembly that will be discussed later. The result of this mechanism is that we can change the blade pitch in a cyclic way (around the azimuth) according to:

$$\theta = \theta_o - A_1 \sin\psi - B_1 \cos\psi \tag{1.5}$$

which means that the pitch of the blade is made out of a common (collective) angle with a lateral (sine) cyclic term and a longitudinal (cosine) term.

At the moment, consider a rotor which is trimmed approximately, with forwards disk tilt caused by longitudinal cyclic pitch. Here we have

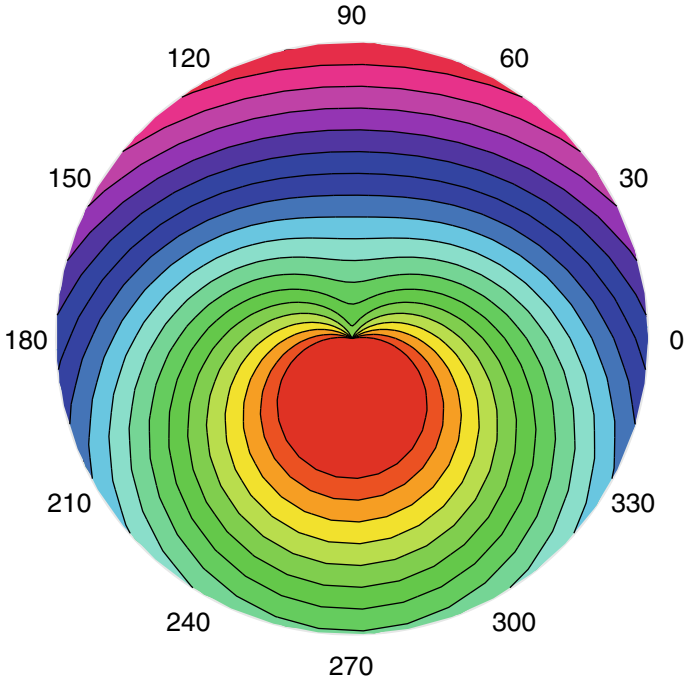

Fig. 1.2 Tangential velocity contours on a rotor disk in forward flight

$$\theta = \theta_0 + B_1 \sin \psi \tag{1.6}$$

The rolling moment coefficient of a rotor in forward flight can be derived from momentum and blade element theories [1]) as

$$C_{MR} = 0.5\sigma a \left[\frac{2}{3}\theta_0 \mu - \frac{B_1}{4}\left(1 + \frac{3}{2}\mu^2\right)\right] \tag{1.7}$$

The lift curve slope a is empirically estimated to 5.7/radian for rotor blades. For zero rolling moment if forward flight this gives a first estimate of the cyclic pitch angles needed to trim the rotor. Maximum blade pitch in occurs at 270 °C azimuth. For high forward speed (assume here $\mu = 0.4$) the maximum pitch can be set close to the blade section stall angle to exploit the maximum performance of the blade section. If a typical static stall angle for a around 15 °C is used we have:

$$15 = \theta_0 + B_1 \tag{1.8}$$

and setting the moment to zero while eliminating the collective from the above equation gives approximately $\theta_0 = 7.5$ degrees and for the longitudinal cyclic pitch we now have $B_1 = 6.5$ degrees. Using these approximations for a rotor in forward flight balances the tendency of the rotor to roll and results in the lift contours shown below.

In actual flight the rotor blades flap up and down in addition to the cyclic pitch. A typical longitudinal trim calculation process for a medium weight helicopter is given by Newman [1]. For a given all up weight (AUW) and fuselage drag at a given airspeed the resultant main rotor thrust vector is fixed in space. This allows calculation of the disk tilt and fuselage tilt angles for moment equilibrium in forward flight. The fuselage drag is available from wind tunnel tests at a reference test speed (usually 100 ft/s or 30.48 m/s). For a medium helicopter this is of the order of D100 = 1000 N. This is scaled to the correct speed using:

$$D_F = D_{100}\left(\frac{U2}{U_{100}^2}\right) = \frac{1000\,U^2}{30.48^2} \tag{1.9}$$

An iteration is performed between the rotor thrust and inflow values to give C_T and $\mu_{zD} = \mu_z + \lambda_i$. This can be done using the MATLAB scripts provided here. The flapping angles (disk tilt), inflow and rotor thrust are input to

$$\begin{bmatrix} \frac{\gamma}{8} & 0 & -\frac{\gamma}{6}\mu_x & -\lambda^2_{\mu_{zD}} \\ 0 & -\frac{\gamma}{8} & 0 & -\frac{\gamma}{6}\mu_x \\ \frac{\gamma}{3}\mu_x & 0 & -\frac{\gamma}{8} & 0 \\ \frac{1}{3}\mu_x & 0 & -\frac{\mu_x}{2} & 0 \end{bmatrix} \begin{bmatrix} \theta_0 \\ A_1 \\ B_1 \\ a_0 \end{bmatrix} = \begin{bmatrix} \frac{\gamma}{6}\mu_{zD} \\ -\frac{\gamma}{8}b_1 + \left(1 - \lambda^2_\beta\right)a_1 \\ -\frac{\gamma}{8}a_1 - \left(1 - \lambda^2_\beta\right)b_1 \\ \frac{C_T}{a\sigma}\frac{\mu_{zD}}{2} \end{bmatrix} \tag{1.10}$$

and this may be used to calculate the collective and cyclic angles, together with the rotor coning angle required for longitudinal trim [2]. In this instance, $\mu_{zD} = \mu_z + \lambda_i$ represents the sum of the climb ratio and downwash. A lateral trim analysis is also necessary due to the amount of cyclic pitch necessary to trim out the effects of tail rotor thrust. In the above, a typical set of data would be $\gamma = 7$, for the blades, that is the Lock number, which is a ratio of aerodynamic to flapping inertia; and $\lambda_{\beta^2} = 1.2$ for a semi-rigid hub, is the non-dimensional flapping frequency, which depends on the rotor hub stiffness and design. A sample longitudinal trim calculation in the speed range of $\mu = 0$ to $\mu = 0.35$ is shown in Fig. 1.3.

With forward speed the fuselage rotates forwards and longitudinal cyclic pitch increases to overcome increasing drag. Of note is the fact that the collective pitch decreases from its hover value to a minimum at around 30 m/s; this is evidence that a rotor in forward flight benefits from "translational lift", which is greater than the lift generated in the hover. However, eventually the increased down-flow through the rotor caused by the forwards disk tilt causes the collective to rise at higher speeds. The longitudinal trim equations are strongly coupled to the lateral trim equations. In lateral trim the procedure is essentially the same, but the tail rotor thrust is also important. These changes in flapping, collective and cyclic angles mean that the rotor blades themselves experience rapid changes in angle of attack as they rotate about the azimuth.

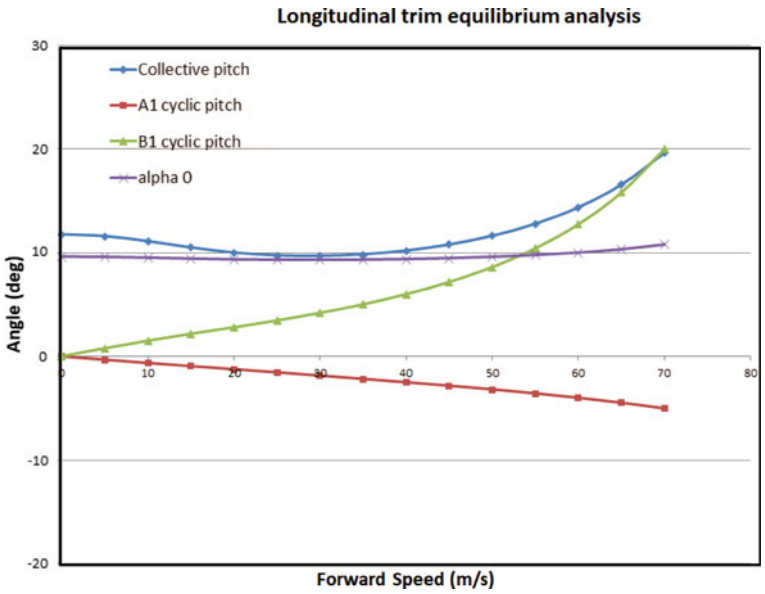

Fig. 1.3 Example of longitudinal rotor trim

1.2.1 Figure-of-Eight Diagram

To determine the aerodynamic environment experienced by a rotor blade in forward flight, a 'sausage plot' is used (sometimes called a 'figure of eight' diagram). This is a plot of blade incidence versus Mach number and shows the range of conditions experienced by the rotor at each station. The blade experiences a very severe aerodynamic environment in forward flight. The advancing blade Mach number towards the tip is very high and in the transonic regime while the retreating blade incidence is close to, or above, the static aerofoil section stall angle. This environment leads to conflicting requirements for the selection of an aerofoil, or for the design of a new rotor section. The high advancing side Mach numbers require thin uncambered sections to prevent drag divergence due to compressibility effects (shock formation). The high lift on the retreating side needs good performance at high angles of attack. The best shape for this task is a thick cambered section but this is not easily achievable. Other design aspects of the helicopter also have conflicting requirements (e.g. twist is desirable for good hover performance, but undesirable in forward flight, or large anhedral at the tip of the rotor blade for hover, and low for forward flight). Moreover, blade aeroelasticity should also be taken into account because blades are relatively flexible in torsion and the aerofoil section must therefore have very low pitching moment. The challenge is to design a blade which has good performance in both of these high Mach and high incidence regimes. These design requirements, and aerofoils which meet them, are discussed next.

To generate a figure-of-eight diagram, one has to start from the basic equations for the blade pitch and flap angles given below.

$$\theta = \theta_0 - A_1 \cos\psi - B_1 \sin\psi, \qquad \text{Blade pitch} \tag{1.11}$$

$$\beta = \beta_0 - a_1 \cos\psi - b_a \sin\psi, \qquad \text{Flap angle} \tag{1.12}$$

As stated earlier, the tangential velocity at the rotor is $U_t = U_{tip}[r_x + \mu \sin(\omega t)]$ and, we must add the effect of blade flapping to the expression for the perpendicular velocity component as:

$$U_p = U_{tip}\left[\lambda_i + \mu\beta\cos(\psi)\right] + r\dot{\beta} \tag{1.13}$$

The inflow angle of air to the blade is $\tan\phi = U_p/U_t$, and we can use ϕ to estimate the angle of attack at a blade section using $\alpha = \theta - \phi$. At the same time, the Mach number at a blade station located a a fraction r_x from the centre is given by $M = M_{tip}(r_x + \mu \sin(\omega t)$.

For a given station r_x and given the properties of the rotor needed for trimming, and after estimating the downwash λ_i using iterative computations we can obtain the sectional angle of incidence α. A plot of the (M, α) will give the "sausage plot" or "figure of eight plot". A typical high speed plot for the Lynx helicopter is shown in Fig. 1.4.

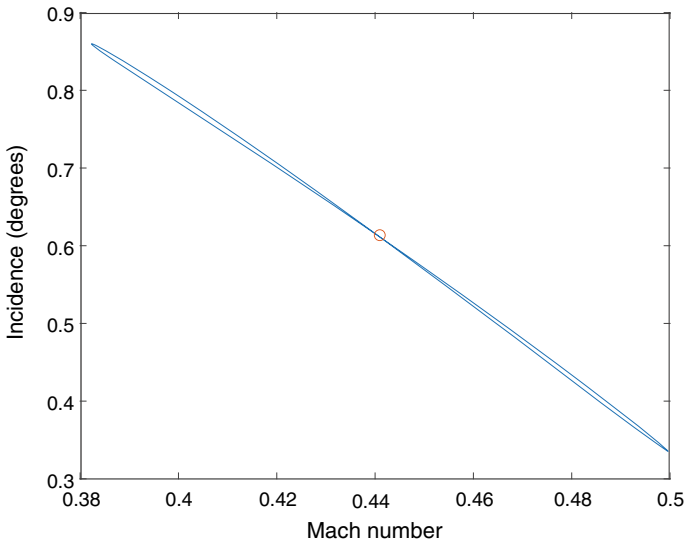

Fig. 1.4 Mach incidence variation of a rotor section at $y/R = 0.75$ and $\mu = 0.1$

1.3 Rotorcraft Aerofoil Sections—History and Current Trends

In the UK, Peter Wilby is perhaps the father of the rotorcraft aerofoil studies. His work included aerofoil design, shape representation aerodynamic performance studies and extensive testing of rotorcraft aerofoils using different wind tunnels. His 1997 Cierva lecture [3] remains relevant today and is a recommended starting point on the topic along with his 1996 paper presented at the European Rotorcraft Forum [4] or his comprehensive work on Vertica [5].

The environment experienced by rotor blades in high speed, forward flight can be summarized by very high incidences, which approach aerofoil stall, on the retreating side and very high Mach numbers on the advancing side. It is these two aerodynamic phenomena, aerofoil stall and shock wave formation, that impose a limit to the forward speed of any helicopter. Rotor blades are high aspect ratio structures. They benefit from a large amount of centrifugal stiffening in blade bending (and flapping motion) but the blade flexibility in torsion is relatively low. Pitching moments associated with stall, transonic effects, or normal rotor operation must be avoided if the blades are not to twist in flight. Initially, symmetric airfoils were used in rotor design and this was by large influenced by the autogyro development where Juan de la Cierva was the first person to use a cambered airfoil section.

A crash in 1939 was blamed on the pitching moments generated by the employed section. Combined with low torsional blade stiffness of early rotors meant that the use of symmetric sections was almost universal until the 1960s. It was only in the 1970s s when progress with computer-based methods allowed for more detailed aerodynamic studies to be performed. Panel methods were first used to allow for iterative studies and implementation of conformal mapping to computer codes was also pivotal. Re-introducing cambered sections was only a matter of time, and this was accelerated by tools allowing the study of transonic flow effects. Ambition with design in the USA and the advent of some high performance helicopters made the aerofoil selection a hot topic of research in the late 1970s. As an example the YAH-64 aircraft that was initially planned to have NACA sections on its blades employed a very advanced, for the time, Hughes HH-02 blade section. (Fig. 1.5)

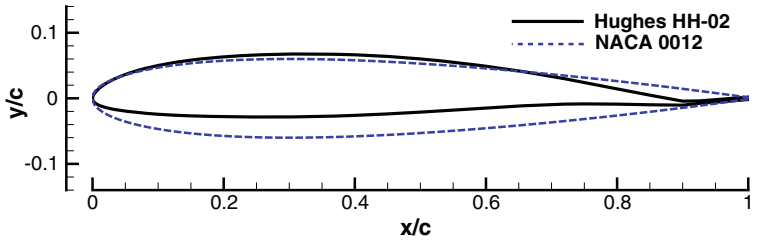

Fig. 1.5 An improved aerofoil section over the NACA series for the blade of the YAH-64 aircraft was the Hughes HH-02 compared with the NACA 23012

Fig. 1.6 Long pitch-links used on rotor heads. The pitch links will suffer higher loads for high-moment aerofoils used on the rotor. Credits: http://www.grubby-fingers-aircraft-illustration.com/

The loss of lift occurring during retreating blade stall is not a major problem. At high forward speed, where retreating blade stall occurs, most of the rotor lift is generated over the fore and aft sectors of the rotor disk at around 60–90% rotor radius so a loss in lift on the retreating blades does not degrade rotor performance significantly. However, there is a large pitching moment change associated with aerofoil stall. This pitching moment change places a large oscillatory load on the blades and their pitch control mechanism. The pitch control linkages may be damaged, or their fatigue life decreased, by retreating blade stall. As a result of these pitching moment loads, retreating blade stall has to be avoided up to as high an advance ratio as possible (Fig. 1.6).

There are two strategies for the aerofoil designer to delay blade stall. One is to increase the blade chord (and hence rotor blade area) and this will decrease the amount of collective pitch, and resulting maximum blade incidence, required to trim the rotor. This strategy can only be used within reason because increased blade chord results in increased profile drag and increased rotor power requirements. Also, blade mass, and the required transmission system mass, increases too. In helicopters rotor design, one of the primary factors for selecting blade chord is to avoid retreating blade stall at VNE (velocity-not-to-exceed). The second strategy is to introduce aerofoil camber so that the blade will reach higher incidences before moment stall. Blade camber is, however, an undesirable feature on the advancing blade where transonic effects are important. In transonic flow, camber can induce strong shock waves with a large drag rise and pitching moment change (Fig. 1.7).

Following Wilby's work, a cambered aerofoil in transonic flow as experienced by the advancing blade will show large pitching moment changes. In transonic flow, the airflow over the upper surface of any aerofoil accelerates to supersonic velocity

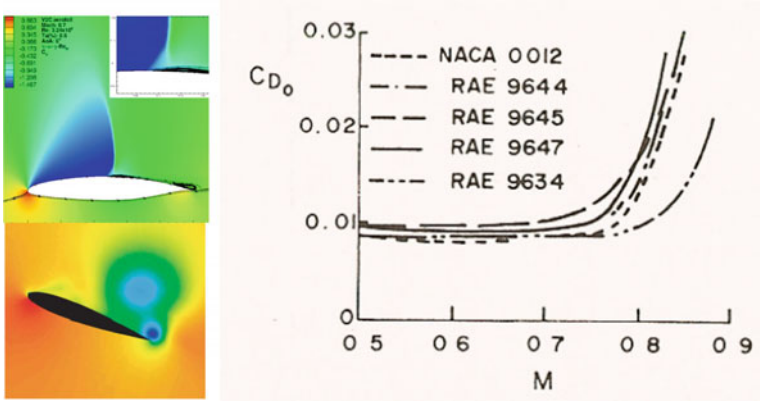

Fig. 1.7 The demanding advancing and retreating side aerodynamics used on the rotors requires sections that can handle Mach flows (outboards where shock waves form) and high-α. Graph on the right from Wilby [5]; graph on the left from Barakos et al. [6]

and forming shock wave recovers to free stream pressure at the trailing edge. The strength and position of this shock wave has a major influence on the amount of transonic drag rise and pitching moment change experienced by the aerofoil. At high forward speed the advancing blade tip is at almost zero incidence (and zero lift). A symmetrical section at zero lift at a Mach number $M = 0.8$ has zero pitching moment, but a cambered section has a strong nose down pitching moment (Fig. 1.8).

The effects of this large, camber-induced, pitching moment on the advancing blade tips can be severe and so the rotor blade and section is designed to minimize the root pitching moment on the advancing blade. The next figure illustrates the problem and shows the torsional load (represented by $M^2\, C_m$) for a cambered and a symmetrical tip aerofoil around the azimuth (Fig. 1.9).

It is evident that the cambered section will produce a large once-per-rev oscillatory load each time the advancing blade passes 90 °C azimuth. The loads are very high, despite the fact that aerofoil stall is not encountered in this example. It is for this reason that the symmetric NACA 0012 section was used for many years as the basic rotor blade section. This aerofoil, albeit simple, has reasonably high stall incidence, low pitching moment and tolerable transonic effects.

1.3.1 Modern Aerofoil Developments

The NACA 0012, and NACA 23012, form the basis of several modern rotor blade sections developed by the National Physics Laboratory (NPL) and the Royal Aircraft Establishment (RAE) in the UK. If a basic NACA 0012 section is used with an extended and drooped leading edge as a means to introduce camber then the resulting aerofoil (e.g. the NPL 9615) can give a 10% increase in C_{Lmax} with a small increase

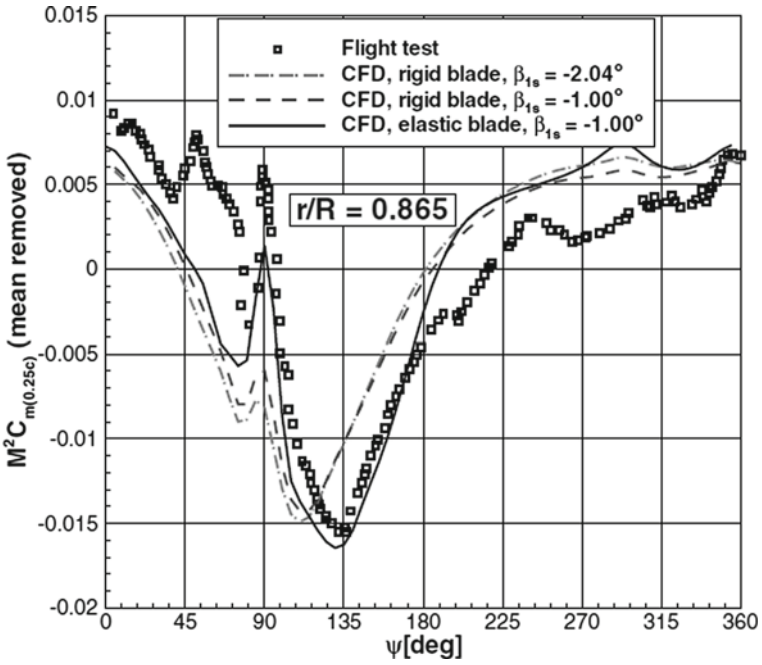

Fig. 1.8 Variation of the blade sectional moment around the azimuth. The figure compares detailed experiments for the UH60A aircraft with simulations using the HMB3 flow solver [7]

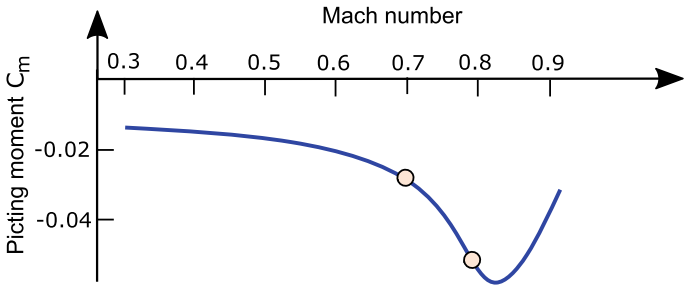

Fig. 1.9 Typical variation of sectional pitching moment coefficient C_m with the Mach number

in Mach number and an acceptable pitching moment at zero lift. Essentially, the nose droop allows an increase in camber without increasing the curvature of the upper surface of the aerofoil and hence avoids the increase in upper surface shock wave strength normally associated with aerofoil camber. The allowable amount of nose droop using this design strategy is limited by the nose down moment that occurs from the underside suction peak (and possible shock wave) resulting from the droop. The introduction of aerofoil camber by this method is illustrated in Fig. 1.10.

Fig. 1.10 Photograph of the RAE 9648 section. ©Getty Images, Science and Society Picture Library

As reported in Wilby's Cierva lecture, research into what pitching moments are sustainable on a rotor was undertaken by the UK RAE on a Wessex helicopter fitted with modified blades (roughened leading edges over certain sections of the blade span). These innovative flight tests at RAE Bedford demonstrated that C_{Lmax} over the inner sections (0 to 60%) of the blades of a helicopter is not a major factor in determining rotor performance and setting the helicopter flight envelope. This is a useful design guideline, because it means that an aerofoil section with reflex camber (an upwards sloping trailing edge for example) and a nose up pitching moment but with poor C_{Lmax} can be used on the inner section of the blades to balance the nose down moment generated by high-lift cambered aerofoil sections further outboard. The modern blade design strategy is therefore to incorporate a modest amount of blade camber on outboard blade sections to delay retreating blade stall, while maintaining low pitching moments and control loads with the use of reflex camber on inboard sections. The NPL 9615 is an example of an early 'modern' rotor aerofoil achieving high lift but with good transonic behaviour. Further research has led to even better section designed by a combination of experience, tunnel testing (at ARA Bedford, and Glasgow University) and numerical methods at RAE and Westland Helicopters (indicial methods by Beddoes) in the RAE 9645 section which is used as the main lifting aerofoil on the Lynx helicopter.

1.3.2 BERP Rotor Aerofoils

The result of many years of tunnel testing (using oscillatory pitching tests to reflect the changing incidences met by rotor blades) and development from the original RAE/NPL 9615 section is a set of three aerofoils each used for a different purpose on the Lynx BERP rotor. RAE 9645 is the main lifting aerofoil used on the Lynx helicopter and is employed between 65 and 85% blade span. This aerofoil is used to achieve the best possible retreating blade stall behaviour. To determine the section's retreating blade stall behaviour, the section is tested in conditions similar to those found on a retreating Lynx blade. A close approximation to these conditions is obtained in a wind tunnel at $M = 0.3$, and where the aerofoil model undergoes sinusoidal pitching 30 Hz and 8 °C half-amplitude. This frequency is selected to obtain a similar reduced frequency $\omega c/U$ between test conditions and real life. An aerofoil

undergoing such oscillations experiences dynamic stall—where the change in pitching moment can be as much as 500% of the static stall moment break. The magnitude of the pitching moment break is plotted against the maximum aerofoil incidence in a cycle and the resulting intercept with the incidence axis is a measure of the maximum achievable blade incidence on the rotor.

This aerofoil has a moderate nose down moment at zero lift resulting from its 'nose droop' camber and so its pitching moment on the rotor blade is balanced by a RAE 9648 section inboard, from the hub up to 65% rotor radius. The RAE 9648 is also 12% thick but has a reflexed trailing edge providing a nose up moment. There is a penalty in using this aerofoil at high Mach numbers because of the lower critical Mach number introduced by reflex camber- however, this is not as important for the inboard sections because their Mach numbers are not too high, even at high advance ratio. Finally a tip aerofoil section, the RAE 9634 is used between 85 and 100% span. This aerofoil is designed to delay transonic flow effects and, consequently, it is only 8.3% thick. Sweeping the tip is another strategy used on modern helicopters to delay transonic effects and this along with the overall planform will be discussed in the next section.

1.4 Planform Effects on Rotor Performance

Following from the aerofoil selection, the rotor planform is now the focus of this paragraph. The rotor can always be seen as a wing in constant rotation and lessons learnt from fixed wings can at least partially be applied to rotary wings. Having mentioned the problems arising due to the drag associated with the formation of shock waves, and considering that the outer part of the rotor will suffer more from compressibility effects due to its higher Mach number, the concept of swept blade tips was first explored by rotor designers. Much the same way the swept wing is used in fixed wing aircraft, applying blade tip sweep can help alleviate some of the problems due to shock formation. However, the alleviation of the shock comes with some drawbacks. First of all the centre of pressure shifts rearwards, and the same happens for the inertial axis the mass of the blade tip. This results in a strong nose-down moment that must somehow be dealt with. One mitigation is to apply moderate amounts of sweep and this may work because the advancing side Mach numbers are not very high. This can be observed in Fig. 1.11, where the AW139 and the Boeing AH64A blade tips are shown. Sweep also results in poor retreating blade performance due to early stall.

A typical aerodynamic envelope for a rotor can be seen in the following figure in the form of a loading versus speed diagram. Clearly, there are two limits to the rotor due to the stall on the retreating side and the compressibility effects of the advancing side. As a result the flight envelope is not significantly improved. It is rather stretched to higher speed but not essentially expanded. This is the reason that many radical ideas for planform shapes have been explored using both CFD and experiments (Fig. 1.12).

(a) AW139 (b) AH64-A

Fig. 1.11 Blade tips of the AW139 and AH64-A helicopters. Credits: **a** https://b-domke.de/AviationImages; **b** https://www.airforce-technology.com

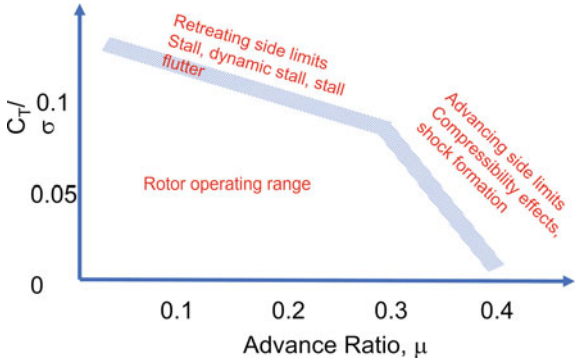

Fig. 1.12 Loading versus advance ratio plot showing the advancing and treating side limitations for conventional rotors

Simply adding sweep will push the speed higher but this will come with reduced lifting capability. A good example of planform design is the British Experimental Rotor Project (BERP). It was a very successful UK (government and industry) programme to develop a much more sophisticated swept tip which would (uniquely) perform well at both high Mach and high incidence. It has a non uniform sweep, incorporates extra frontal area (which counters the aft movement of the centre of pressure), and has a very highly raked tip.

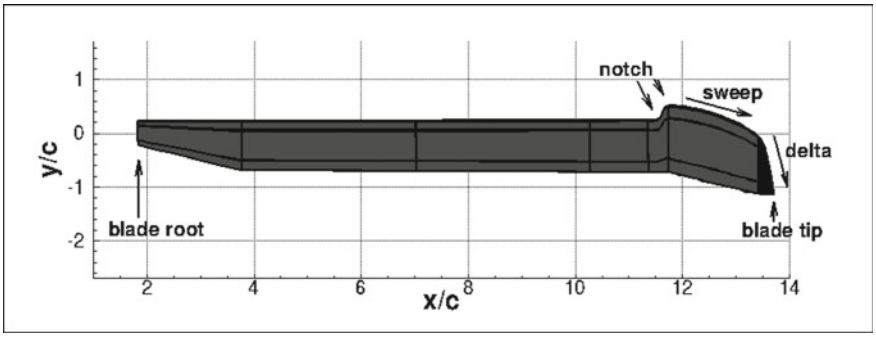

Fig. 1.13 Definition of the parameters of the BERP-like blade

1.4.1 BERP Blade

The BERP blade has a "paddle-shaped" tip due to a forward displacement of the planform (creating a notch) followed by sweep as shown in Fig. 1.13.

It is a benchmark design because of its improved performance in forward flight resulting in a world speed record for helicopter flight [8]. Some CFD analysis was carried out for this blade in order to find the specific reasons for its improved performance, and to analyse what happens in the flow field around it [9]. However, at the time, computational power was limited and today, higher fidelity CFD methods are available. The aim of this chapter is to apply CFD and optimisation methods to investigate if further performance can be obtained by fine-tuning specific features of the BERP tip. At the same time, the methods outlined in the literature survey chapter of this book are applied.

The BERP tip was designed for high speed forward flight without compromising hover performance [10]. The problem associated with the fast forward flight regime, is that the effects of compressibility such as transonic flow and shock waves become significant especially on the advancing blade. Typically, thin aerofoils are used but these tend to stall more easily at the high angles of attack which occur on the retreating side. The first step in the design of the BERP was the aerofoil selection. The aerofoils were selected such that thinner sections could be used to enable higher forward flight speeds. Camber was introduced to improve the stall capability of the blade on the retreating side and the increased pitching moments were alleviated by having a reflexed aerofoil inboards. The resulting blade is reported to behave well in terms of control requirements and twist loads [11].

The planform was then optimised to reduce high Mach number effects by first sweeping the tip of the blade back. This moved the aerodynamic centre of the swept part backwards, causing control problems in the pitch axis. To counteract this, the swept part was translated forward which introduced a notch on the leading edge of the blade. The notch corners were smoothed to avoid flow separation. A "delta" tip

was also incorporated so that a stable vortex formed at higher angles of attack on the retreating side to delay stall [9].

One of the characteristics of the blade is that blade stall occurs first inboards of the notch and does not spread outwards. This is because at high angles of attack, such as at the retreating side, the vortex formed travels around the leading edge and the flow over the swept part remains attached. The BERP blade shows similar performance to a standard rotor blade at low speed flight, but superior performance in forward flight due to the absence of drag rise and flow separation [9]. In hover, the Figure of Merit (FM) was improved due to the minimisation of blade area and overall, there were no penalties in hover performance. At high speeds, blade vibration was also reduced as well as control loads for manoeuvres [9].

BERP(3) is currently in use on the Lynx and Merlin helicopters. J. Perry was the main driver behind this project that resulted in a "paddle" tip at the end of the blades. At first the twist of the blades was not uniformly applied but was stronger near the tips to provide the necessary off loading without resulting to too high pitch angles inboard. Then the tip was swept in a non-uniform way so that in hover the Mach number is kept constant along the tip. The shape near the tip is almost like a delta wing, highly raked, and inboard a notch was created increasing the chord and forming the paddle shape. The notch also helps offset the CP aft movement resulting in a more balanced shape with lower pitching moments. At high pitch the notch can also result in an additional vortex helping the tip to stay free from stall at high loading and α.

This design helps so that tips do not stall until a high angle and shock waves are delayed to higher speed. The selection of the tip speed was dictated by a requirement to keep the Mach number $M < 0.88$ at the advancing side to stay below the drag divergence of the employed tip sections.

The advance ratio was also kept below 0.4 so that dynamic stall effects can be tolerable. In hover, the Mach had to be less than 0.7 to avoid shock waves and divergence of drag. Lower limits of speed were set by auto-rotation considerations; this gave a speed of 210 m/s at 160 kt.

The tip speed was decided using several criteria. To begin with,

$$U_{tip} < M_{crit}\sqrt{\gamma RT} - U_{flight} \tag{1.14}$$

In Eq. 1.14, $\gamma = 1.4$, R is the gas constant and T is the absolute temperature. This means that the tip Mach number is below the critical Mach number for the aerofoil used at the tip of the blade. At the same time the dynamic stall of the retreating side should be controlled and this means restricting the advance ratio to about 0.4, or $0.4U_{tip} > U_{flight}$. The hover tip Mach number is also kept low so that the blades operate near max incidence with no shock wave development. This is around 0.68, or $U_{tip} < 0.68\sqrt{\gamma RT}$. The restrictions lead to a map like the one presented in Fig. 1.14.

The blade chord is a difficult selection given that blade area is needed so that stall is avoided especially near the maximum advance ratio. For this case, rotor stability is very important and at the same time the designer has to consider an advance ratio

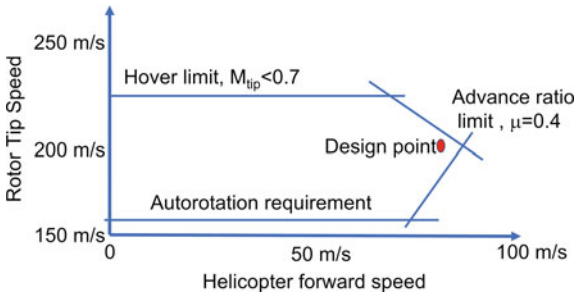

Fig. 1.14 Tip-speed considerations during design

that is above limits set by High pitch link loads, stall flutter, and stability. Thus, lowering the blade incidence requires increasing the blade chord. The blade are is usually selected so that maximum C_T/σ is not exceeded.

$$A_{blade} = \left(\frac{C_T}{\sigma}\right)^{-1} \frac{W}{\rho\,(\Omega R)^2} = 10\,\mathrm{m}^2 \tag{1.15}$$

Selecting different disk loading and specific power loading is also important and the take-off where power is high. Hence, selecting a disk loading and according to the engine characteristics we find out the intersection of power loading vs disk loading with the take-off requirement.

The selection of the number of blades is also interesting. More blades lead to less vibration so dynamics and vibration of the rotor is crucial At the same time good manoeuvrability leads to stiff hubs. Keeping the complexity of the hub low is also important so more than 5 blades increases the complexity. It appears that 4 or 5 blades is the optimum for medium helicopters with light helicopters at times even opting for 3 blades. More blades are usually seen in very heavy helicopters.

1.5 Modern Rotor Design, Methods and Approaches

The design of rotor blades is complex, in that it involves many disciplines of engineering such as aerodynamics, structural dynamics, aeroelasticity and flight control systems. These disciplines do not just play an individual part in the design of the rotor blade, but are coupled; some more strongly than others [12]. Even within a single discipline, such as the aerodynamics of the rotor, there are often conflicting design requirements; Forward flight tends to have opposite requirements to hover, the blade on the advancing side has opposite requirements to that on the retreating side of a forward moving helicopter and so on [13]. Therefore, defining an optimum blade tends to be a compromise between these various conditions. Hence, the optimum is determined by the objectives set for each particular rotor design. While the initial

rotor design may be relatively easy to come up with, finding the optimum design parameters is not an easy task.

For the named reasons, computer codes to aid helicopter designers have been, and are still being, developed and used in the industry [14]. In the past, these methods were limited to using simple theories that modelled the aerodynamics of a rotor. This limitation was due to the high cost in obtaining sufficient data to make valid comparisons for a set of design parameters, either by experiments or by simulation. Both methods involve high costs. The computational costs, however, can be reduced by reducing the complexity of the models used to simulate the aerodynamics around a rotor. However, this compromises the accuracy of the data. Nevertheless, over time, computing power has increased allowing more advanced simulation models to be used. This has attracted a lot of interest in the research of design and optimisation methods.

A variety of methods have been developed, and the majority of the applications have been for cases that require a small computational domain (such as aerofoils) or a simple aerodynamic analysis (such as cases where operation is optimised for a single static condition). The challenge is to apply these methods to a complex design such as a helicopter rotor blade, where the aerodynamics are complex and change, and the design space has a large number of dimensions, and to do this accurately and efficiently. The initial concept design is a well-established process and designers and engineers of rotor blades have substantial experience to lean on, as well as the assistance of efficient codes to aid them in obtaining a preliminary rotor design. The optimisation methods become more applicable when optimisation of an existing design is required to obtain even better performance from a rotor.

Optimisation techniques usually require a starting design point, so the design stage is just as important as the optimisation. While it is possible for optimisation to lead to new designs, the time and effort involved would attract a high cost. Take the BERP tip blade as an example [10]. The BERP tip blade is not something that can easily be created by using optimisation methods. However, if the designer's ideas and experience in the field of aerodynamics was used to create an initial design, then the dimensions and extent of the BERP blade characteristics can be perfected to improve performance. When many characteristics of a rotor are adjusted in such a way, a considerable amount of improvement can be made [13]. This is what makes optimisation so important and has led to the increase in the amount of research conducted and the number of academic papers written on this topic.

Alongside the added performance gained by using optimisation procedures, the use of numerical solutions for the optimisation problem removes some of the workload of obtaining the optimum design from the designer while still giving the designer flexibility. In the case of rotors specifically, there are many criteria and objectives that must be fulfilled simultaneously, what is known as multi-objective optimisation. Depending on the required performance, it is possible to program the optimiser to create a rotor tailored to its expectations in many diverse conditions.

The challenge of optimisation for helicopters is summarised in the following quote from Ref. [15]:

"Researchers in helicopter applications of optimisation face a complex multi disciplinary problem, with several possible choices of design variables, objective functions, behavior and side constraints, analysis models, sensitivity formulations, approximation concepts, optimisation algorithms, not to mention the many types of results that can be generated and presented."

References

1. Newman S (1994) Foundations of helicopter flight. Arnold, Great Britain
2. Seddon J (1990) Basic helicopter aerodynamics. BSP Professional Books, Great Britain
3. Wilby PG (1998) Shockwaves in the rotor world–a personal perspective of 30 years of rotor aerodynamic developments in the UK. Aeronaut J 3:113–128
4. Wilby PG (1996) The development of rotor Aerofoil testing in the UK—the creation of a capability to exploit a design opportunity. Proc Eur Rotorcraft Forum, (Paper no 18):18–1–18–11
5. Wilby PG (1980) The aerodynamic characteristics of some new RAE blade sections, and their potential influence on rotor performance. Vertica 4:121–133
6. Barakos GN, Drikakis D (2003) Computational study of unsteady turbulent flows around oscillating and ramping Aerofoils. Int J Fumer Methods Fluids 42:163–189. https://doi.org/10.1002/fld.578
7. Steijl R, Barakos GN, Badcock KJ (2008) Computational study of the advancing-side lift-phase problem. J Aircraft 45(1):246–257
8. Perry FJ, Wilby PG, Jones AF (1998) The BERP rotor–how does it work, and what has it Beein doing lately. Vertiflite 44(2):44–48
9. Brocklehurst A, Duque EPN (1990) Experimental and numerical study of the british experimental rotor programe blade. In: AIAA 8th applied aerodynamics conference, vol AIAA-90-3008, Portland, Oregon, USA
10. Harrison R, Stacey S, and Hansford B (2008) BERP IV the design, development and testing of an advanced rotor blade. In: American helicopter society 64th annual forum, Montreal, Canada
11. Robinson K, Brocklehurst A (2008) Berp iv—aerodynamics, performance and flight envelope. In: 34th European rotorcraft forum, Liverpool, UK
12. Caradonna FX (1992) The application of CFD to rotary wing problems. In: NASA Technical Memorandum
13. Gordon Leishman J (2005) Principles of helicopter aerodynamics. Cambridge Aerospace Series, 2nd edn
14. Johnson W (2010) NDARC—NASA design and analysis of rotorcraft validation and demonstration. In: American Helicopter society aeromechanics specialist conference, San Francisco, California
15. Celi R (1999) Recent applications of design optimization to rotorcraft—a survey. In: 55th annual forum of the American helicopter society

George Barakos is at the School of Engineering, Glasgow University, where he specialises in high-fidelity aerodynamics and aero-acoustics models, computational fluid dynamics, high-performance computing and rotorcraft engineering.